Quantum Size Effects in Adatom Island Decay

Karina Morgenstern,[1] Erik Lægsgaard,[2] and Flemming Besenbacher[2,1]

[1]*Institut für Festkörperphysik, Universität Hannover, Appelstrasse 2, D-30167 Hannover, Germany*

[2]*Department of Physics and Astronomy, and Interdisciplinary Nanoscience Center (iNANO), University of Aarhus, DK-8000 Aarhus C, Denmark*

(Received 24 January 2005; published 29 April 2005)

The decay of hexagonal Ag adatom islands on top of larger Ag adatom islands on a Ag(111) surface is followed by a fast-scanning tunneling microscope. Islands do not always show the expected increase in decay rate with decreasing island size. Rather, distinct quantum size effects are observed where the decay rate decreases significantly for islands with diameters of 6, 9.3, 12.6, and 15.6 nm. We show that electron confinement of the surface state electrons is responsible for this enhancement of the detachment barrier for adatoms from the island edge.

DOI: 10.1103/PhysRevLett.94.166104 PACS numbers: 68.35.Fx, 68.37.Ef, 73.20.At, 82.20.Xr

Thin metal films and small quantum dots have a wide range of applications in modern technologies. Quantum size effects are found to occur when the size of the nanostructure becomes comparable to the de Broglie wavelength of electrons confined within it. Such confinement effects have profound implications on various nanoscale physical properties.

The first observation of quantum size effects in individual islands was made for Pb islands on Cu(111) [1], where it was shown that preferred heights occur for islands without quantum well states close to the Fermi level [2]. Also Ag and Pb thin films on semiconductor substrates showed magic heights [3–6]. The detection of quantum states was extended towards thinner films, and a correlation between the electronic property and the thickness of an individual island was demonstrated [7]. It has been proposed that the competition between quantum confinement, charge spilling, and interface-induced Friedel oscillation defines the existence of the characteristic magic thicknesses [8]. Thus, in a so-called ''electronic growth'' mode for metals on semiconductors, the energy contribution of quantized electrons confined in the metal overlayer determines the morphology of the growing film, and this energy contribution prevails over the strain energy. This insight was used to tune the surface reactivity of magnesium films towards oxidation [9]. It was also observed that annealing of the Pb overlayer on Cu(111) [10] and the Ag overlayer on Fe(100) [11] leads to magic layer thicknesses associated with quantum size effects. All these observations originate from the confinement of electrons normal to the surface, and it was implicitly assumed that the extension of the macrostructure was too large in the lateral direction to produce lateral confinement. However, electron confinement of the surface state electrons in the lateral dimension leads to quantum interference patterns on nanoscale islands. These patterns were observed in both homoepitaxial [12] and heteroepitaxial [13] systems.

During the initial growth of adatom islands, the system is out of equilibrium due to a supersaturation caused by evaporation. When nucleation and growth are terminated, atoms flow from steps with high curvature to steps with low curvature, making small islands shrink, while large islands grow at their expense. This coarsening process, referred to as Ostwald ripening, is a general feature and it also occurs between islands in different layers. The adatom motion between islands of different layers is different from the adatom motion for islands within the same layer due to the so-called Enrich-Schwoebel (ES) barrier [14]. Atoms that detach from the top island have to overcome this additional energy barrier before they can be incorporated into the bottom island. While the understanding of Ostwald-ripening processes between islands in the same layer has advanced significantly in recent years for metals [15,16] as well as for semiconductors [17], the ripening between islands on different layers has not been investigated thoroughly, although postannealing of three-dimensional films is often used as a simple way of forming smooth surface layers. Only one specific aspect of the ripening between layers has attracted a lot of interest [18], since it has been shown that, on Cu(111) and Ag(111) surfaces, ripening increases by orders of magnitude when the distance between the island edges falls below a critical width [18–23]. On Cu(111) it is found that this critical distance coincides with the distance where the surface state is depopulated. For Ag(111), however, the critical distance for the occupation of the surface state is far above the experimentally determined critical width [21–23]. Thus these observations cannot be explained by quantum size effect, and the underlying mechanism is still under intense debate [24].

In this Letter, we show how lateral electron confinement influences the decay of individual adatom islands, resulting in distinct quantum size effects. We have studied in detail the decay of islands adsorbed concentrically on top of larger islands. By means of fast-scanning STM, we find a transition between attachment-limited decay for large islands, where the decay is determined by the interface to the bottom island, and diffusion-limited decay for smaller islands, where the decay is dominated by the ability of

 © 2005 The American Physical Society

the adatom to diffuse to the next sink. The shift between these two limiting regimes can be well understood within an ordinary continuum model and is caused by the increasing distance between the two step edges of the top and bottom islands during the decay. Very surprisingly, we find that the island decay is reduced significantly at certain island sizes. We relate these distinct island sizes to the absence of quantum well states near the Fermi level and conclude that the energy barrier for adatom detachment depends on the quantum confinement of electrons. Thus, we present the first observation of the influence of electron confinement onto surface kinetics.

The experiments were performed on Ag(111) single crystal surfaces, which were cleaned by 1 keV Ar^+ sputtering for 30 min and annealing to ~650 °C for 30 min. Several sputter-anneal cycles were followed by a final flash to ~850 °C, leading to terraces with a width larger than 1000 nm. Up to 7 ML (monolayers) of silver was deposited with a rate between 0.3 and 0.8 ML/min, resulting in stacks of adatom islands [25]. The subsequent change in morphology of the islands during annealing experiments was recorded by means of the home-built variable-temperature Aarhus STM and visualized in the form of so-called STM movies, i.e., sequences of time-lapsed STM images [26]. As in earlier similar studies, special precaution was taken to avoid any influence of the scanning STM tip [25]. The microscope is operated in a standard ultrahigh vacuum system (base pressures of 5×10^{-11} Mar) that was equipped with standard surface science techniques for sample preparation and characterization. The high thermal stability of the STM combined with a special, active thermal drift-compensated routine allowed us to follow dynamically the morphological changes on surfaces over extended time periods (> 13 h) [25].

After obtaining stable imaging conditions, the dynamic coarsening of the islands was followed by repeatedly scanning the same spot of the surface. Figure 1(a) shows the decay of the top layer of a four-layered Ag island at 330 K. This particular island shows the decay characteristics expected for island decay in the diffusion limit: The decay rate smoothly increases with decreasing island size. Often, however, the decay curves exhibit regions in which the decay proceeds at a slower rate [Figs. 1(b) and 1(c)]. This decrease in decay rates occurs at specific island sizes, e.g., for the island in Fig. 1(b) at ≈ 80 nm^2. In this example, the lower adatom island gets smaller during the island decay. Figure 1(c) demonstrates that the decreased decay rates also occur for a lower island, whose area is increasing.

Before discussing the decreased decay rates, we will discuss the shape of the decay curves aside from the plateaus. The decay of adatom islands on terraces [19,27] follows a functional dependence of the island area A on time of $A = a(t_0 - t)^{2b}$. The decay exponent b, obtained by fitting this power law to the island in Fig. 1(a), varies continuously from $b = (0.27 \pm 0.01)$ for the total curve over (0.29 ± 0.02) from $t > 1000$ s to (0.3 ± 0.1) from $t > 1500$ s. The last part of the decay curve for the island in

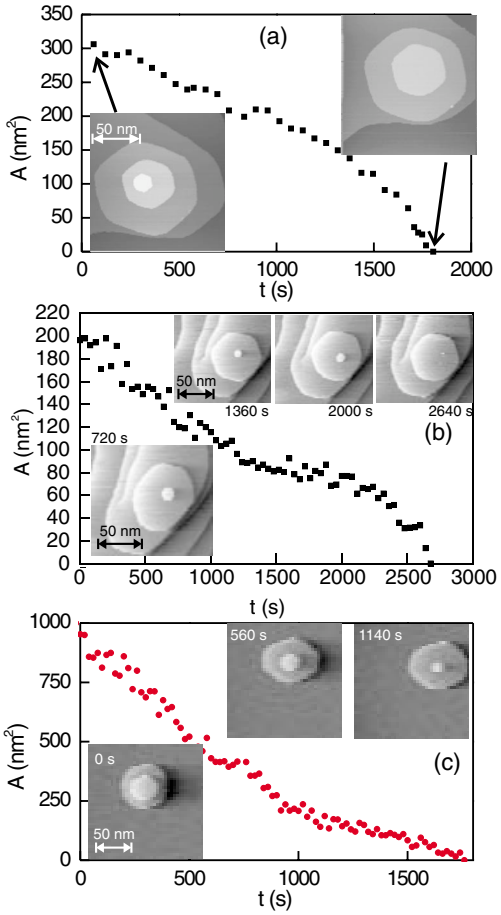

FIG. 1 (color online). Area development in time for decay of the top-layer island of different adatom island stacks; STM images are snapshots of the STM movie at the indicated times. Parameters are (a) the initial size of bottom island $A_R = 2500$ nm^2, tunneling current $I = 40$ pA, sample voltage $U = 2$ V, measurement temperature $T = 330$ K; (b) $A_R = 3500$ nm^2, $I = 5$ nA, $U = 0.3$ V, RT; (c) $A_R = 2800$ nm^2, $I = 1.5$ nA, $U = -1$ V, RT.

Fig. 1(b) has a decay exponent, which increases continuously from 0.2 (considering the last 1500 s) to ≈ 0.25 for the last 1000 s to >0.3 for the last 500 s. This variation in the decay exponent with island size is in variance with previously observed fixed exponents for island decay on terraces or within vacancy islands [18,19,27–31].

We account for the varying decay exponent by solving the diffusion equation in an ordinary continuum description, which has already been used with success to describe the decay of adatom and vacancy islands within large vacancy islands and on large terraces [19,25,27]. In this model, we consider the geometry sketched in Fig. 2(a) [25]: A small adatom island of radius r is placed concentrically on top of a larger adatom island of radius R. The decay of the top-layer island can be described by the three net fluxes indicated in Fig. 2(a): (i) the flux of adatoms from the adatom island to the terrace J_r, (ii) the diffusion flux of adatoms over the terrace $J_{r \to R}$, and (iii) the attach-

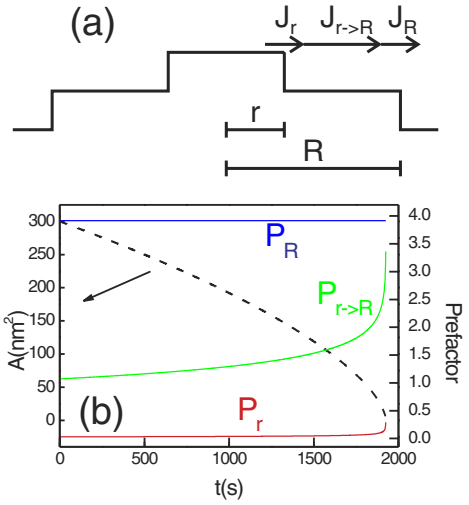

FIG. 2 (color online). (a) Theoretically considered scenario; for details, see text. (b) Decay curve from integration for the island in Fig. 1(a) (dashed line) with the value of prefactors as indicated (solid lines); integration values: $A_R = 2560$ nm^2, $E_s = 0.13$ eV, $E_e = 0.71$ eV, $\gamma = 0.75/\text{nm}$, $T = 330$ K.

ment flux of adatoms to the outer island J_R. Considering mass conservation and the equality of net fluxes at steady state in analogy to the theoretical modeling of a vacancy island within a vacancy island [19] yields a differential equation for the island area $A = \pi r^2$:

$$\frac{dA}{dt} = -\frac{2\pi D}{n}\frac{\rho_{\text{eq}}(r) - \rho_{\text{eq}}(R)}{P_r + P_{r\to R} + P_R}, \tag{1}$$

where n is the atomic density in the surface layer, D is the diffusivity of adatoms over the surface, and $\rho_{\text{eq}}(\hat{r}) = \rho_\infty \exp(\gamma/kTn\hat{r})$ is the equilibrium adatom concentration of a step of curvature $1/\hat{r}$ with k the Boltzmann constant and T the absolute temperature. The prefactors $P_r = a/r$, $P_{r\to R} = \ln(R/r)$, and $P_R = a/Rs$ result from the three net fluxes involved [Fig. 2(a)], with a the surface lattice constant and $s = s_0 e^{-E_s/kT}$, with E_s the ES barrier.

P_r is by far the smallest term for our experimental configuration, reaching at most a tenth of P_R, and it is therefore negligible [$E_s = 0.13$ eV, $s_0 = 0.25$ for Ag(111)] [19]. The relative importance of the other two terms changes during the decay. A dominance of P_R is indicative of an attachment-limited decay; i.e., the decay kinetics is dominated by the ability of atoms to attach to the bottom island. If, however, $P_{r\to R}$ dominates, the decay is diffusion limited; i.e., the decay kinetics is dominated by the diffusion of the adatoms between the island edges.

We can linearize the exponential expressions for the adatom concentrations of Eq. (1) and thereby obtain an analytical solution in the attachment-limited case ($P_R \gg P_{r\to R}$) which yields $A = a(t_0 - t)^{2b}$ with an invariable decay exponent of $b = 1/3$. However, the increasing importance of the diffusion-limited term for decreasing island size results in a mixture of the two decay regimes, and thus in a variety of "apparent" decay exponents, in accordance with our experimental observation. A correct description of the experimental data in principle demands numerical integration of Eq. (1), as is shown in Fig. 2(b) for the experiment of Fig. 1(a) using the material parameters of Ag(111) determined previously [19]. Discrepancies in the decay time to the experimental data in Fig. 1(a) result from deviations from the concentric geometry in the experiment. The increasing importance of the diffusion-limited term is evident from the increasing value of the prefactor $P_{r\to R}$.

The island size $\tilde{r}$ at which the decay will be predominantly diffusion limited ($P_R < P_{r\to R}$) is given by

$$\tilde{r} = Re^{a/Rs}. \tag{2}$$

The type of island decay depends thus on the sizes of the two islands involved (r and R) and the Ehrlich-Schwoebel barrier, i.e., the material and specific crystal face.

The continuum theory thus explains the observed continuous variation of the decay exponent. It cannot, however, explain the observed decrease in decay rate at certain distinct island sizes [Fig. 1(b)]. Such apparent decay plateaus are observed for many islands for lower island sizes varying from 150 to 10 000 nm^2 regardless of whether the lower island grows or decays. In Fig. 3(a) we show some more decay curves. These reveal a distinct reduction in the decay rate by approximately 1 order of magnitude for different islands at certain island sizes. Although the different islands show plateaus at similar values, not all decay curves show plateaus at all the characteristic island size values.

In Fig. 3(b) we have plotted the diameter from the decay curves measured at fixed time intervals for several islands in a histogram. Distinct preferred sizes are observed for island diameters of 6, 9.3, 12.6, and 15.6 nm. These peaks correspond to those island diameters, where the decay rate is much slower than expected from the continuum treatment.

For the vertical growth mode reported in [2], the island heights with no quantum well states at the Fermi level are preferred. In the lateral dimension, magic island sizes without quantum well states of the surface state electrons near the Fermi level are given approximately by $\lambda_F/4 + n(\lambda_F/2)$, with $\lambda_F/2 = 3.7$ nm for Ag(111), which leads to 5.55, 9.25, 12.95, and 16.65 nm for $n = 1, \ldots, 4$. The comparison to the maxima in Fig. 3(b) reveals a clear correlation between the size of the stabilized islands and these values.

Thus, we have shown that the island decay slows down whenever there is no quantum well state near the Fermi level. This implies that not only the total energy of an island oscillates as a function of its size, as in electronic growth [1–9], but also the energy barrier for detachment does so.

From the comparison of the decay rates, in the "regular" decay regime and the decreased decay rates we can estimate the energy difference of this detachment barrier

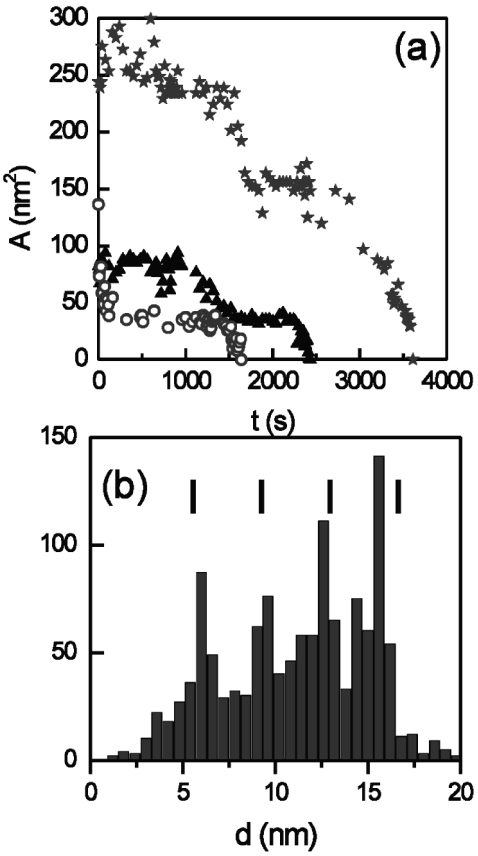

FIG. 3. (a) Areas of several top-layer islands decaying at RT. (b) A histogram of measured island sizes for 10 different islands. Island sizes have been measured every 10 s; diameters are calculated disregarding the straight edges of the islands (this introduces only a minor error [25]); vertical bars indicate island sizes, which have no quantum well state at the Fermi level (see text).

(under the assumption of the same prefactor) to (0.07 ± 0.03) eV. This is about one-tenth of the total detachment rate, which was determined in a different decay experiment to 0.7 eV [19].

In conclusion, the study of the dynamics of the top layer of a multilayered adatom island stack on Ag(111) with a fast-scanning tunneling microscope reveals two remarkable phenomena: a transition from attachment-limited to diffusion-limited decay, and a quantum size effect in island kinetics. Both phenomena are expected not to be restricted to the particular system. The former is important whenever the island sizes are close to fulfilling Eq. (2). The latter will influence island decay for all surfaces with occupied surface states.

We acknowledge stimulating discussions with Roberto Otero. One of us (K. M.) acknowledges support by the Deutsche Forschungsgemeinschaft.

[1] B. J. Hinch, C. Koziol, J. P. Toennies, and G. Zhang, Europhys. Lett. **10**, 341 (1989).
[2] R. Otero, A. L. Vazquez de Parga, and R. Miranda, Phys. Rev. B **66**, 115401 (2002).
[3] A. R. Smith, K.-J. Chao, Q. Niu, and C.-K. Shih, Science **273**, 226 (1996).
[4] I. B. Altfeder, K. A. Matveev, and D. M. Chen, Phys. Rev. Lett. **78**, 2815 (1997).
[5] L. Huang, S. J. Hay, and J. H. Weaver, Surf. Sci. **416**, L1101 (1998).
[6] L. Gavioli, K. R. Kimberlin, M. C. Tringides, J. F. Wendelken, and Z. Zhang, Phys. Rev. Lett. **82**, 129 (1999).
[7] W. B. Su, S. H. Chang, W. B. Jian, C. S. Chang, L. J. Chen, and T. T. Tsong, Phys. Rev. Lett. **86**, 5116 (2001).
[8] Z. Zhang, Q. Niu, and C.-K. Shih, Phys. Rev. Lett. **80**, 5381 (1998).
[9] L. Aballe, A. Barinov, A. Locatelli, S. Heun, and M. Kiskinova, Phys. Rev. Lett. **93**, 196103 (2004).
[10] J. H. Dil, J. W. Kim, S. Gokhale, M. Tallarida, and K. Horn, Phys. Rev. B **70**, 045405 (2004).
[11] K. L. Man, Z. Q. Qiu, and M. S. Altman, Phys. Rev. Lett. **93**, 236104 (2004).
[12] J. Li, W. D. Schneider, R. Berndt, and S. Crampin, Phys. Rev. Lett. **80**, 3332 (1998).
[13] S. Pons, P. Mallet, and J.-Y. Veuillen, Phys. Rev. B **64**, 193408 (2001).
[14] G. Ehrlich and F. G. Hudda, J. Chem. Phys. **44**, 1039 (1966); R. L. Schwoebel and E. J. Shipsey, J. Appl. Phys. **37**, 3682 (1966).
[15] K. Morgenstern, G. Rosenfeld, and G. Comsa, Surf. Sci. **441**, 289 (1999).
[16] G. Schulze Icking-Konert, M. Giesen, and H. Ibach, Surf. Sci. **398**, 37 (1998).
[17] W. Theis, N. C. Bartelt, and R. M. Tromp, Phys. Rev. Lett. **75**, 3328 (1995).
[18] M. Giesen, G. Schulze Icking-Konert, and H. Ibach, Phys. Rev. Lett. **80**, 552 (1998).
[19] K. Morgenstern, G. Rosenfeld, E. Lægsgaard, F. Besenbacher, and G. Comsa, Phys. Rev. Lett. **80**, 556 (1998).
[20] M. Giesen, G. Schulze Icking-Konert, and H. Ibach, Phys. Rev. Lett. **82**, 3101 (1999).
[21] K. Morgenstern, G. Rosenfeld, G. Comsa, E. Lægsgaard, and F. Besenbacher, Phys. Rev. Lett. **85**, 468 (2000).
[22] M. Giesen and H. Ibach, Surf. Sci. **464**, L697 (2000).
[23] K. Morgenstern, G. Rosenfeld, G. Comsa, M. R. Sœrensen, B. Hammer, E. Lægsgaard, and F. Besenbacher, Phys. Rev. B **63**, 045412 (2001).
[24] M. I. Larsson, Phys. Rev. B **64**, 115428 (2001).
[25] K. Morgenstern, Phys. Status Solidi B **242**, 773 (2005).
[26] F. Besenbacher, Rep. Prog. Phys. **59**, 1737 (1996).
[27] K. Morgenstern, G. Rosenfeld, and G. Comsa, Phys. Rev. Lett. **76**, 2113 (1996).
[28] D. R. Peale and B. H. Cooper, J. Vac. Sci. Technol. A **10**, 2210 (1992).
[29] J.-M. Wen, J. W. Evans, M. C. Bartelt, J. W. Burnett, and P. A. Thiel, Phys. Rev. Lett. **76**, 652 (1996).
[30] J. B. Hannon, C. Klünker, M. Giesen, H. Ibach, N. C. Bartelt, and J. C. Hamilton, Phys. Rev. Lett. **79**, 2506 (1997).
[31] A. Ichimiya, Y. Tanaka, and K. Ishiyama, Surf. Sci. **386**, 182 (1997).